narra j

Original Article

Inhibition of B-cell activating factor activity using active compounds from *Physalis angulata* in the mechanism of nephrotic syndrome improvement: A computational approach

Astrid K. Kardani[1,2,3*], Loeki E. Fitri[4,5*], Nur Samsu[6,7], Krisni Subandiyah[2,3], Agustina T. Endharti[8], Dian Nugrahenny[9] and Syahputra Wibowo[10]

[1]Doctoral Program in Medical Sciences, Faculty of Medicine, Universitas Brawijaya, Malang, Indonesia; [2]Division of Nephrology, Department of Pediatric, Faculty of Medicine, Universitas Brawijaya, Malang, Indonesia; [3]Division of Nephrology, Department of Pediatric, Dr. Saiful Anwar General Hospital, Malang, Indonesia; [4]Department of Clinical Parasitology, Faculty of Medicine, Universitas Brawijaya, Malang, Indonesia; [5]Department of Clinical Parasitology, Dr. Saiful Anwar General Hospital, Malang, Indonesia; [6]Division of Nephrology, Department of Internal Medicine, Faculty of Medicine, Universitas Brawijaya, Malang, Indonesia; [7]Division of Nephrology, Department of Internal Medicine, Dr. Saiful Anwar General Hospital, Malang, Indonesia; [8]Department of Parasitology, Faculty of Medicine, Universitas Brawijaya, Malang, Indonesia; [9]Department of Pharmacology, Faculty of Medicine, Universitas Brawijaya, Malang, Indonesia; [10]Eijkman Research Center for Molecular Biology, National Research and Innovation Agency (BRIN), Bogor, Indonesia

*Corresponding authors: astridkardani@student.ub.ac.id (AKK) and lukief@ub.ac.id (LEF)

Abstract

Nephrotic syndrome, a multifaceted medical condition characterized by significant proteinuria, has recently prompted a reorientation of research efforts toward B-cell-mediated mechanisms. This shift underscores the pivotal role played by B-cells in its pathogenesis. The aim of this study was to explore potential therapeutic pathways, with specific attention given to compounds found in *Physalis angulata*, including withanolides, such as physalins, which constitute one of the five distinct withanolide subgroups identified in *Physalis angulata*. Furthermore, the study assessed the monoclonal antibody belimumab, designed to target B-cell activating factor (BAFF) and its associated receptors (TACI, BCMA, and BAFF-R). Various research techniques were employed, encompassing data mining, bioactivity analysis, Absorption, Distribution, Metabolism, Excretion, and Toxicity (ADMET) profiling, molecular modeling, and docking studies. Withanolide was demonstrated as a potential inhibitor for the protein BAFF, showing a binding energy of -7.1 kcal/mol. Physalin F emerged as the leading candidate inhibitor for the protein TACI, with a binding energy of -8.3 kcal/mol. Similarly, withanolide was identified as the top inhibitor candidate for the protein BCMA, exhibiting a binding energy of -7.0 kcal/mol. The most favorable interaction with BAFF-R was physalin F, which displayed a binding energy of -8.0 kcal/mol. Moreover, molecular dynamic simulation suggested that physalin F was able to maintain protein stability, hence being a good inhibitor candidate for BAFF-R and TACI proteins. The results of this investigation demonstrated substantial promise, indicating that these withanolides and withaphysalin A compounds derived from *Physalis angulata* offer alternative avenues for B-cell targeting. Consequently, this study presents opportunities for pioneering treatments in the management of nephrotic syndrome.

Keywords: BAFF, physalin, physalin F, nephrotic syndrome, withanolide

https://narraj.org/

Received: May 13, 2024 - Accepted: June 24, 2024 - Published online: September 5, 2024

Introduction

Nephrotic syndrome is a clinical syndrome distinguished by significant proteinuria, resulting in low levels of albumin, generalized edema (anasarca), high lipid levels, and a variety of other associated complications [1]. Currently, there is a change in the way we understand the origins of idiopathic nephrotic syndrome. The traditional idea of immune response dysregulation in the glomerular basement membrane is being replaced by a focus on podocyte injury or podocytopathy. This podocyte damage can occur through immune or non-immune mechanisms [2]. Podocytes are undeniably the central target cells in the immune system mechanism responsible for inducing podocyte injury in nephrotic syndrome. While the role of T-cells in nephrotic syndrome pathogenesis has been widely acknowledged, there is currently a shifting belief that B-cells also play a pivotal role in its development [3].

Pescovitz *et al*. documented cases of recurrent focal segmental glomerulosclerosis (FSGS) following transplantation that experienced remission after receiving B-cell depletion therapy in the form of rituximab, originally intended for addressing post-transplant lymphoproliferative disease (PTLD). Subsequently, numerous case reports and clinical trials have emerged concerning B-cell depletion therapy aimed at sustaining long-term remission in nephrotic syndrome patients. The increased number of activated B-cells in patients with idiopathic nephrotic syndrome (INS) significantly decreases following remission [4]. This effectiveness indicates B-cell involvement in podocyte injury and underscores its pivotal role in the pathogenesis of INS [5]. When discussing the role of B-cells in the context of INS, recent studies have unveiled that the expression of B-cell activating factor (BAFF) in the podocytes of pediatric patients suffering from nephrotic syndrome is correlated with unfavorable renal outcomes [6]. Additionally, an investigation examined the levels of BAFF in the serum of patients with IMN undergoing treatment with prednisone, cyclophosphamide, rituximab, and belimumab. Notably, patients receiving supplemental rituximab and belimumab therapy exhibited diminished BAFF levels in comparison to the cohort exclusively administered prednisone and cyclophosphamide therapy [6]. These findings underscore the involvement of BAFF and its associated receptors in the immune responses of pediatric nephrotic syndrome patients [6-7].

B-cell activating factor (BAFF) is a vital cytokine in the maturation and differentiation of B-lymphocytes, which is known to possess three receptors: transmembrane activator and CAML interactor (TACI), protein maturation of B-cells (BCMA), and BAFF-receptor or BR-3 (BAFF-R). The clinical application of BAFF as a nephrology biomarker has recently garnered considerable attention [2]. BAFF and its three receptors have been acknowledged for their significant roles in other immune-related disorders, such as systemic lupus erythematosus (SLE) [8]. Consequently, the involvement of B-cells in nephrotic syndrome designates them as a promising target for novel therapeutic approaches. Nonetheless, the use of belimumab and rituximab, while demonstrating a favorable long-term safety profile, is also associated with the notable risk of serious complications, particularly infections stemming from neutropenia [9].

Due to these complications, an alternative solution that could present a breakthrough is the utilization of plant extracts in the context of nephrotic syndrome. The focus on belimumab as a control in this research is because belimumab is a monoclonal antibody that works by targeting B-cell activating factor (BAFF). Therefore, its activity can be directly compared with that of active compounds. *Physalis angulata* is recognized for its various pharmacological activities, including anti-inflammatory and immunosuppressive properties. In a lupus rodent model, *Physalis angulata* has been observed to subdue immune responses. *Physalis angulata* contains several active compounds, such as phytosteroids like withanolides A and B, physalins B, D, and F, physagulins C, D, and A, as well as flavonoids like quercetin, ursolic acid, and lupeol [10]. Withanolides and physalins are the two main active constituents frequently used in various studies, and they are known for their anti-inflammatory effects [10,11]. It is worth emphasizing that within withanolides, characterized by modified structural configurations, there exist five distinct subgroups. These subgroups encompass physalins, neophysalins, withaphysalins, 14α,20α-epoxides, and ring-D aromatic withanolides. Physalins and neophysalins, in particular, are notably abundant in oxygenation and can manifest a C-14–C-27 oxygen bridge. Importantly,

physalins and neophysalins are intricately linked by a biogenetic relationship with the broader withanolide class [11-12].

The presence of withanolides in Indian ginseng is recognized for its potent immunomodulatory effects. Similar to the benefits of withanolides in Indian ginseng, *Physalis angulata* is also known to exhibit potent immunomodulatory effects by suppressing B-cell proliferation, macrophage activation, and cytokine production [13]. In conjunction with methylprednisolone, *Physalis angulata* extract has demonstrated the potential to alleviate inflammation and enhance renal function in a lupus rodent model [12]. This is due to regulations of inhibiting NF-kB signaling, mitigating excessive immune responses, and reducing apoptosis resulting from oxidative stress triggered by an exaggerated immune response. Nevertheless, despite its robust anti-inflammatory and immunosuppressive properties, there is a paucity of research investigating the effects of *Physalis angulata* on nephrotic syndrome. It is speculated that the presence of glucocorticoid receptor transcription factors in BAFF may be one of the mechanisms through which *Physalis angulata* influences BAFF activity, courtesy of the phytosteroid effects exhibited by several of its bioactive components, including withanolides and physalins [13-15]. This study employed bioinformatics techniques to explore the potential of *Physalis angulata* compounds, involving analyses of compound activity, pharmacokinetic properties, molecular modeling, and molecular docking, all aimed at elucidating the extract's impact on BAFF protein activity.

Methods

Data mining

The compounds utilized in the in silico analysis were obtained from the PubChem database, with the respective PubChem IDs as follows: 14216298 (withaphysalin A), 6384266 (physalin), 433531 (physalin F), 53477765 (withanolide), and 11294368 (withanolide A). The selection of these compounds is based on the research conducted by Brar *et al*. and Timotius *et al*. [16,17], where it was established that the predominant components of *Physalis angulata* encompass withapysalin, withanolides and physalins in a general sense. Specifically, among these constituents, physalin F stands out prominently. The control drug is belimumab (5Y9J). As for the proteins used, their sequences were sourced from the NCBI protein database. The proteins employed in the study were TACI *Homo sapiens* (BAE16555.1), B-cell activating factor *Homo sapiens* (AAD25326.1), BCMA *Homo sapiens* (BAB60895.1), and BAFF-R *Homo sapiens* (BAE16554.1).

Bioactivity analysis of compounds

The activity of the bioactive molecules was predicted using the Way2Drug software, which can be accessed at https://www.way2drug.com/passonline. The chemical Simplified Molecular Input Line Entry System (SMILES) notation for each compound was obtained from the PubChem database, corresponding to the PubChem ID for each substance. The data selected for analysis met specific criteria, with a requirement of Pa>0.7.

Absorption, distribution, metabolism, excretion, and toxicity (ADMET) analysis

In drug development, ADMET encompasses the absorption, distribution, metabolism, excretion, and toxicity of compounds. In silico ADMET profiling serves as a vital tool for anticipating the pharmacological and toxicological attributes of potential drugs, especially during the early stages of research. These computational models focused on enhancing ADMET predictions, are pivotal in optimizing drugs and averting late-stage setbacks. Such failures not only consume substantial time and financial resources but can also be avoided by leveraging these predictive models. The experimentation in this study harnessed the capabilities of pkCSM-pharmacokinetics.

The pkCSM-pharmacokinetics web tool (https://biosig.lab.uq.edu.au/pkcsm/) introduces a pioneering approach to forecast and optimize the ADME/Tox attributes of small molecules. This method relies on the incorporation of graph-based signatures and experimental data.

Molecular modelling

Computational methods have long been utilized to predict 3D structures in the absence of experimental data. AlphaFold, a noteworthy application of deep learning algorithms in biomedicine, has significantly revolutionized the field of structural biology. AlphaFold 2 accommodates input from both the protein sequence and a template structure. The target's sequence is retrieved from the NCBI database, and a Google Colab (https://colab.research.google.com/github/sokrypton/ColabFold/blob/v1.2.0/AlphaFold2.ipynb) is employed to predict the 3D structure based on this sequence.

Protein assessment

To assess the model's quality, we applied geometric and stereochemical criteria. This evaluation was carried out using the PDBsum tool, accessible at http://www.ebi.ac.uk/pdbsum. PDBsum plays a critical role in validating PDB structures, focusing on the precision of stereochemistry and the accuracy of the predictive model. The assessment primarily relied on the calculation of the Ramachandran plot, which scrutinizes torsion angles Ø and Ψ within the amino acid residues of proteins. The results were expressed as a percentage, categorizing regions as core, allowed, generously allowed, or disallowed, thus providing a comprehensive measure of the protein structure's quality.

Molecular docking

All ligands were prepared using the Open Babel software, involving energy minimization and format conversion from .sdf to .pdbqt. The docking process was carried out using AutoDock Vina, which is included in the PyRx 0.8 package. AutoDock Vina was chosen for its ability to provide more accurate binding poses compared to AutoDock 4 [18-21]. It is worth noting that the docking parameters varied for each protein. For BAFF, the Vina search box dimensions covered X (138.7164), Y (75.0697), and Z (104.1665), with the center of the box located at X (-1.1414), Y (-6.5055), and Z (0.7897). As for BCMA, the Vina search box dimensions encompassed X (89.4274), Y (70.3385), and Z (108.8155), while the center of the box was positioned at X (-10.459), Y (10.6879), and Z (7.6867). Moving on to TACI, the Vina search box dimensions included X (121.4032), Y (113.5989), and Z (119.8834), and the center of the box was situated at X (5.3673), Y (-9.4113), and Z (1.4070). Lastly, for the BAFF-R protein, the Vina search box dimensions covered X (115.8261), Y (70.8183), and Z (92.9311), with the center of the box located at X (4.0843), Y (1.4188), and Z (-3.1796). For the docking between belimumab and all proteins using ClusPro 2.0 (https://cluspro.bu.edu), the selected binding energy was based on van der Waals and electrostatic energy. Visualization of protein docking with compounds using Discovery Studio Client 2021, while protein-protein interactions utilize PDBSum.

Molecular dynamic simulation

For molecular dynamic (MD) simulation, the CABS-flex 2.0 webserver (http://biocomp.chem.uw.edu.pl/CABSflex2) was used. The targets of this MD were BAFF, BCMA, BAFF-R, and TACI using selected ligands selected through molecular docking with optimal binding affinity. This MD simulation system determined root mean square fluctuation (RMSF) values at 10-ns resolution with 50 cycles and 50 trajectory frames within 10 ns each cycle frame. Additional distance restraints, including global weight of one were applied during the simulation.

Results

Bioactivity of *Physalis angulate* compounds

According to the results from the Prediction of Activity Spectra for Substances (PASS) server (**Figure 1**), it is indicated that withanolide compounds exhibited a probability of functioning as immunosuppressants and oxidoreductase inhibitors. However, data on withanolide A indicated its functions as an antineoplastic, antieczematic, antileukemic, and phosphatase inhibitor. The in silico bioactivity data of withanolide A (**Supplementary data**) was not presented in the main paper because when integrated with molecular docking data, it did not demonstrate the capability

as an inhibitor of the BAFF protein. Physalin F displayed significant biological activities, including antineoplastic and antileukemic effects. Physalin compounds are recognized for their versatile properties, notably as inhibitors of oxidoreductase enzymes.

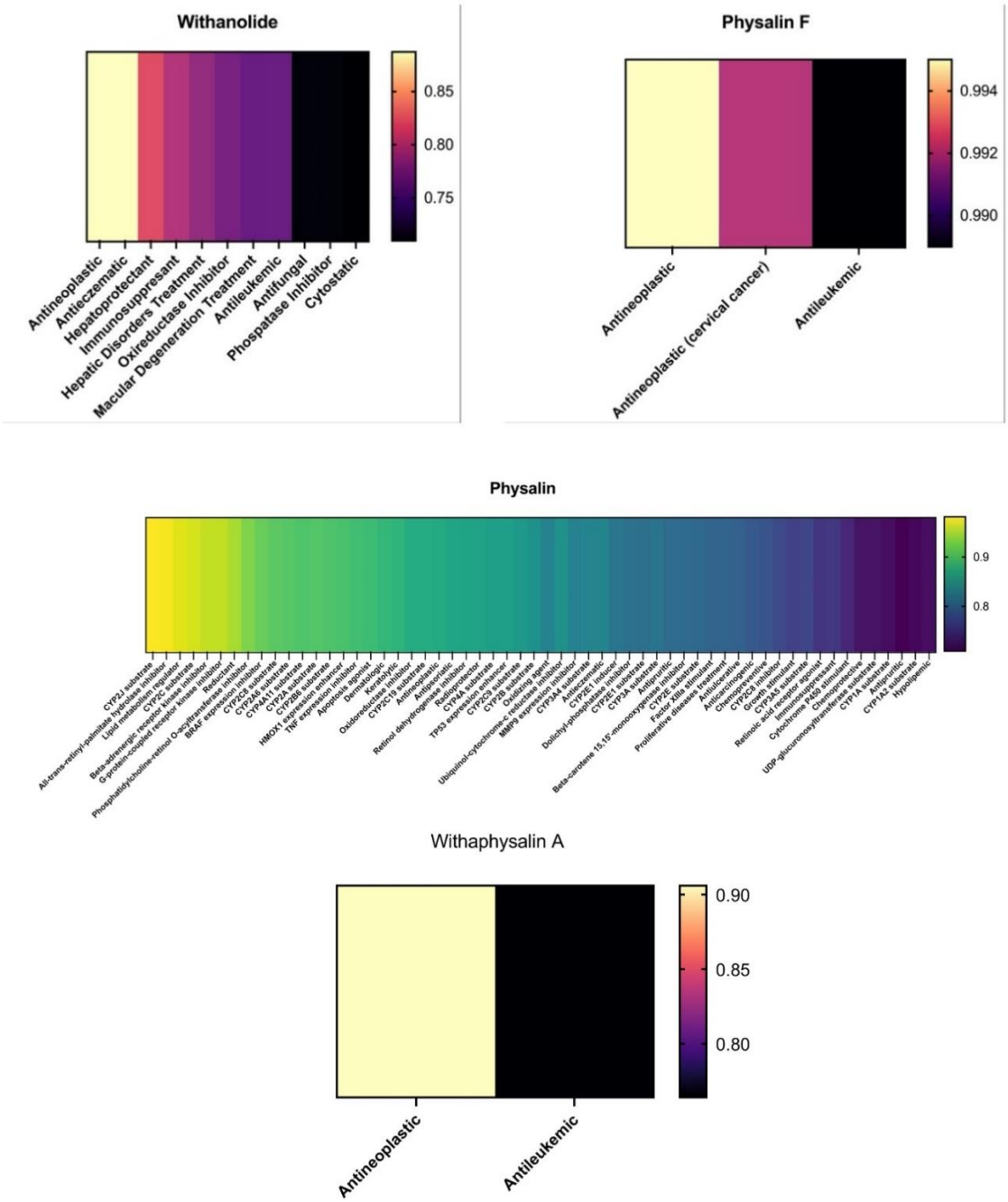

Figure 1. Prediction of Activity Spectra for Substances (PASS) server results.

ADMET of *Physalis angulata*

The categorization of compounds based on Caco-2 permeability, as predicted by the pKCSM model (**Table 1**), is pivotal in assessing their potential for efficient intestinal absorption. Notably, all of the compounds surpassed the 0.90 threshold, indicating high Caco-2 permeability and suggesting a likelihood of robust absorption. In contrast, physalin F fell short of this threshold, signifying lower Caco-2 permeability and potential absorption limitations.

In accordance with the pkCSM guidelines, compounds with less than 30% absorption through the human intestine are considered poorly absorbed. Based on this, the compounds in question can be categorized accordingly. Withanolide, boasting an absorption rate of 80.639%, and physalin, with an absorption rate of 81.744%, both fell within the category of well-absorbed

compounds. This suggested a notable potential for efficient absorption within the human intestinal tract, an attribute of significance in pharmaceutical applications. Furthermore, physalin F, demonstrating a 100% absorption rate, is classified as exceptionally well-absorbed, while withaphysalin A, with 98.421%. Similarly, withanolide A (**Supplementary data**) demonstrated an intestinal absorption rate of 100%. Meanwhile, the absorption based on P-glycoprotein, the compound that can be absorbed in the presence of a P-glycoprotein 2 inhibitor, was physalin, while the one interacting with P-glycoprotein as a substrate was physalin F. In contrast, withanolide did not exhibit any interaction with this protein. Meanwhile, withanolide A (**Supplementary data**) indicated that this compound can interact with all P-glycoprotein types.

Table 1. pKCSM results of withanolide, physalin and physalin F

Property	Model	Unit	Withanolide	Physalin	Physalin F
Absorption	Water solubility	Numeric (log mol/L)	-3.323	-2.905	-4.3
Absorption	Caco-2 permeability	Numeric (log Papp in 10^{-6} cm/s)	2.207	1.332	0.807
Absorption	Intestinal absorption (human)	Numeric (% absorbed)	80.639	81.774	100
Absorption	Skin permeability	Numeric (log Kp)	-2.735	-2.735	-2.725
Absorption	P-glycoprotein substrate	Categorical (Yes/No)	No	No	Yes
Absorption	P-glycoprotein I inhibitor	Categorical (Yes/No)	No	No	No
Absorption	P-glycoprotein II inhibitor	Categorical (Yes/No)	No	Yes	No
Distribution	VDss (human)	Numeric (Fu)	-2.309	-0.788	0.781
Distribution	Fraction unbound (human)	Numeric (logBB)	0.285	0.366	0.255
Distribution	BBB permeability	Numeric (logPS)	0.58	-1.325	-0.998
Distribution	CNS permeability	Categorical (Yes/No)	-1.472	-0.962	-3.086
Metabolism	CYP2D6 substrate	Categorical (Yes/No)	No	No	No
Metabolism	CYP3A4 substrate	Categorical (Yes/No)	No	Yes	Yes
Metabolism	CYP1A2 inhibitor	Categorical (Yes/No)	Yes	No	No
Metabolism	CYP2C19 inhibitor	Categorical (Yes/No)	No	No	No
Metabolism	CYP2C9 inhibitor	Categorical (Yes/No)	No	No	No
Metabolism	CYP2D6 inhibitor	Categorical (Yes/No)	No	No	No
Metabolism	CYP3A4 inhibitor	Categorical (Yes/No)	No	No	No
Excretion	Total clearance	Numeric (log ml/min/kg)	0	1.086	-0.188
Excretion	Renal OCT2 substrate	Categorical (Yes/No)	No	No	No
Toxicity	Ames toxicity	Categorical (Yes/No)	Yes	No	No
Toxicity	Maximum tolerated dose (human)	Numeric (mol/kg/day)	1.414	0.3	-1.513
Toxicity	hERG I inhibitor	Categorical (Yes/No)	No	No	No
Toxicity	hERG II inhibitor	Categorical (Yes/No)	No	No	No
Toxicity	Oral rat acute toxicity (LD_{50})	Numeric (mol/kg)	2.482	2.555	4.576
Toxicity	Oral rat chronic toxicity (LOAEL)	Numeric (log mg/kg bw/day)	0.285	4.124	2.617
Toxicity	Hepatotoxicity	Categorical (Yes/No)	No	No	No
Toxicity	Skin sensitisation	Categorical (Yes/No)	No	No	No
Toxicity	Skin *T. pyriformis* toxicity	Numeric (log ug/L)	0.285	0.285	0.285
Toxicity	Minow toxicity	Numeric (log mM)	4.49	-12.318	4.591

BBB: blood-brain barrier; CNS: central nervous system

VDss is categorized as low when it falls below 0.71 L/kg (log VDss<-0.15) and high when it exceeds 2.81 L/kg (log VDss>0.45). According to these criteria, withanolide (log VDss=-2.039) was classified as having low VDss, indicating a more restricted distribution in the body. In contrast, physalin (log VDss=-0.788) fell within the intermediate range. Meanwhile, physalin F and withaphysalin A (log VDss=0.781 and 0.312, respectively) were categorized as having high VDss, suggesting a wider distribution throughout the body. Furthermore, blood-brain barrier (BBB) permeability was assessed based on a logBB value, where a logBB greater than 0.3 indicates that the compound can readily cross the BBB, while a logBB less than -1 suggests poor distribution

to the brain. Under these criteria, withanolide (logBB=0.58) was anticipated to have good BBB permeability. On the other hand, physalin (logBB=-1.325) was expected to have limited distribution to the brain, while withaphysalin A and physalin F (logBB=-0.226 and -0.998, respectively) fell into the intermediate range.

Lastly, central nervous system (CNS) permeability was evaluated based on the logPS parameter, where a logPS greater than -2 indicates the ability to penetrate the CNS, and a logPS less than -3 signifies an inability to do so. In this context, withanolide (logPS=-1.472) was categorized as having limited CNS permeability. Physalin (logPS=-0.962) fell within the intermediate range. Notably, physalin F and withaphysalin A (logPS=-3.086 and -2.895, respectively) were classified as unable to penetrate the CNS [26]. As for withanolide A (**Supplementary data**), the VDss value of -0.097 indicated that the compound falls within the intermediate range, signifying a relatively balanced distribution throughout the body. Withanolide A possessed a logBB value of -0.255, categorizing it as having limited permeability across the BBB. Additionally, with a logPS value of -2.681, the compound was considered capable of penetrating the CNS.

The evaluation of how a compound interacts with the crucial detoxification enzyme Cytochrome P450 holds profound implications for drug metabolism and effectiveness. Withanolide is classified as a CYP1A2 inhibitor, indicating its potential to influence the metabolism of drugs that are processed by this specific isoform. In contrast, withanolide A (**Supplementary data**), physalin, physalin F and withaphysalin A are recognized as CYP3A4 substrates, implying that they may undergo metabolism mediated by this particular isoform. These observations underscore the significance of comprehending how compounds engage with different Cytochrome P450 isoforms, as these interactions can affect drug activation or deactivation, ultimately shaping their pharmacological characteristics and potential interactions with other drugs [22].

The evaluation of total clearance for withanolide, withanolide A, physalin, and physalin F unveiled distinctive pharmacokinetic characteristics. Withanolide stood out with a total clearance value of 0, signifying limited or negligible elimination from the body. Conversely, physalin demonstrated a moderate clearance rate, as indicated by its value of 1.086, suggesting a well-balanced elimination process. In contrast, physalin F displayed a negative total clearance value (-0.188), implying potential inadequate clearance and the likelihood of accumulation within the body. Withanolide (2.482), physalin (2.555), physalin F (4.576), and withaphysalin A (2.341) exhibited varying degrees of acute toxicity as indicated by their rat LD_{50} values, reflecting potential adverse effects. Regarding hepatotoxicity, all compounds were non-toxic. When considering Ames toxicity, withanolide was categorized as "yes," indicating potential mutagenicity, while physalin, physalin F and withaphysalin A were characterized as "no," suggesting a lower likelihood of causing mutations. In the context of *T. Pyriformis* toxicity, all four compounds, withanolide (0.285), physalin (0.285), physalin F (0.285), and withaphysalin A (0.293), demonstrated similar and relatively low levels of toxicity. However, the minnow toxicity results revealed a notable contrast, with withanolide (4.49) and physalin F (4.591) indicating elevated toxicity levels, while physalin (-12.318) exhibited significantly reduced toxicity [22].

Molecular modelling and assessment

Molecular modelling in this study harnessed AlphaFold 2 (**Figure 2**), successfully generating models for all four proteins (TACI, BCMA, BAFF, and BAFF-R) and the control drug, belimumab. Quality assessment of the BCMA protein, consisting of 184 residues, revealed that 90.9% of the residues were situated within favored and allowed regions, with the remaining 9.1% falling into disallowed regions. These findings indicated the promising quality of the BCMA protein, making it suitable for further analysis.

Moving to the BAFF protein, the quality assessment indicated that 95.2% of its residues were in favored and allowed regions, with only 4.8% in disallowed regions. Similarly, for the BAFF-R protein, 93.3% of the residues were within favored and allowed regions, while 6.7% were found in disallowed regions. As for the TACI protein, with a total of 293 residues, 87.5% of the residues were located in favored and allowed regions, and the remaining 12.5% were in disallowed regions. Importantly, the modelling results consistently displayed favorable patterns across ranks 1 to 5

for TACI, indicating the reliability of the protein models. Meanwhile, belimumab had 99,2% residues in the right place and only 0.8% in disallowed regions. This suggested that these proteins were well-suited for further docking analysis [23].

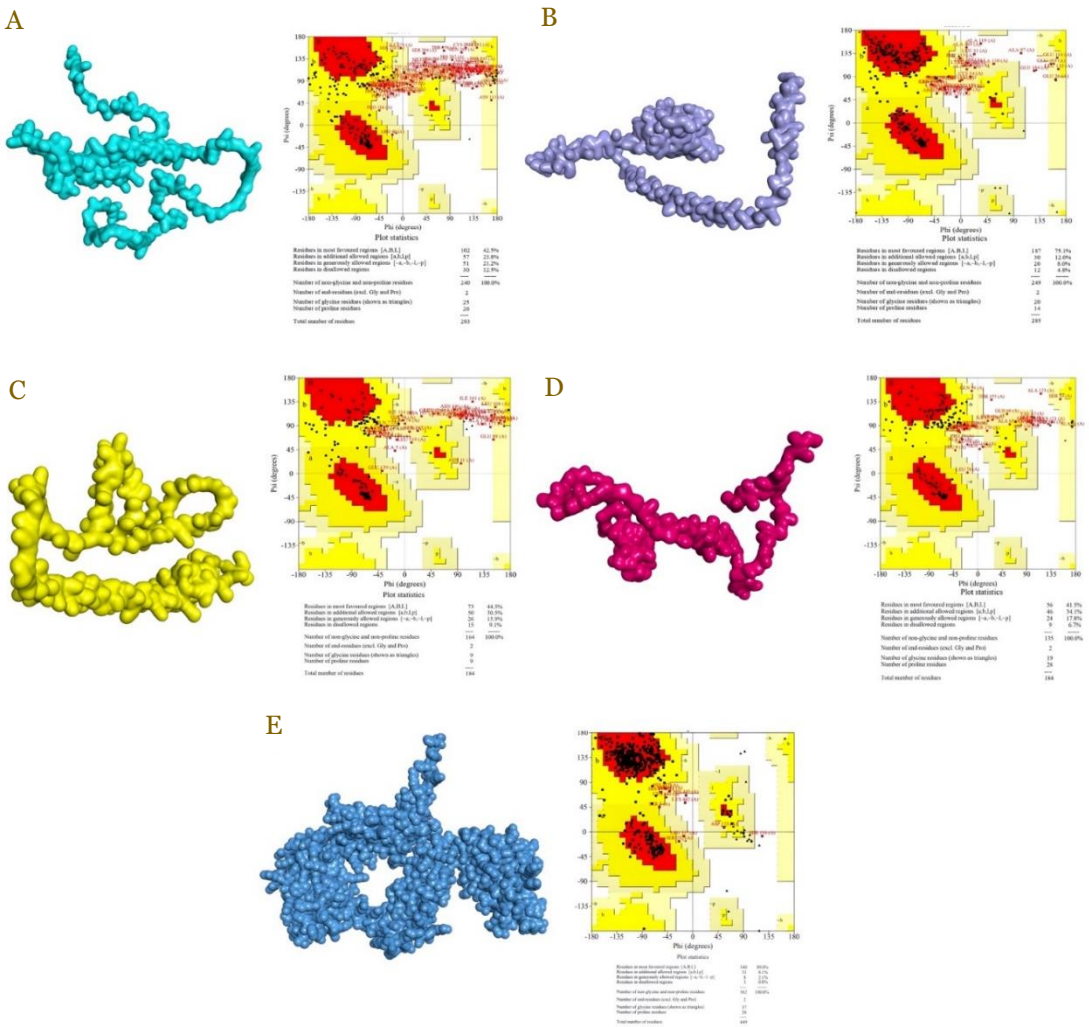

Figure 2. Protein model and assessment of TACI (A), BAFF (B), BCMA (C), BAFF-R (D), and belimumab (E).

Molecular docking analysis

BAFF protein

Based on the docking results (**Figure 3**), belimumab as the control compound (**Figure 3E**), exhibited a binding energy of -259 kcal/mol with 13 salt bridges, 18 hydrogen bonds and 103 non-bonded contacts. Direct comparison of binding energies between protein-protein interactions in the control group and compound-protein interactions in the experimental group was not feasible due to inherent differences in the molecular interactions involved. However, through docking studies, the potential of active compounds from *Physalis angulata* to interact with target proteins could be exlpored, offering promising alternatives for drug development. It is also worth noting that antibody therapies such as belimumab currently entail significant time and cost compared to the extraction of natural compounds.

When assessing the binding energy, physalin F (**Figure 3C**) appeared to have the best energy with -7.2 kcal/mol. However, it is important to note that there are unfavorable donor-donor interactions, a type of binding that can lead to protein instability and may result in the ligand detaching from the protein or even causing protein unfolding, thereby disrupting its function. The compound that emerged as a potential candidate as a BAFF protein inhibitor was withanolide, with a binding energy of -7.1 kcal/mol.

It formed three hydrogen bonds with SER244, ASP275, and TYR246. Withaphysalin A also exhibited inhibitory capabilities similar to physalin F, albeit less effectively in the context of forming stable hydrogen bonds due to possessing only one hydrogen bond at residue THR 157.

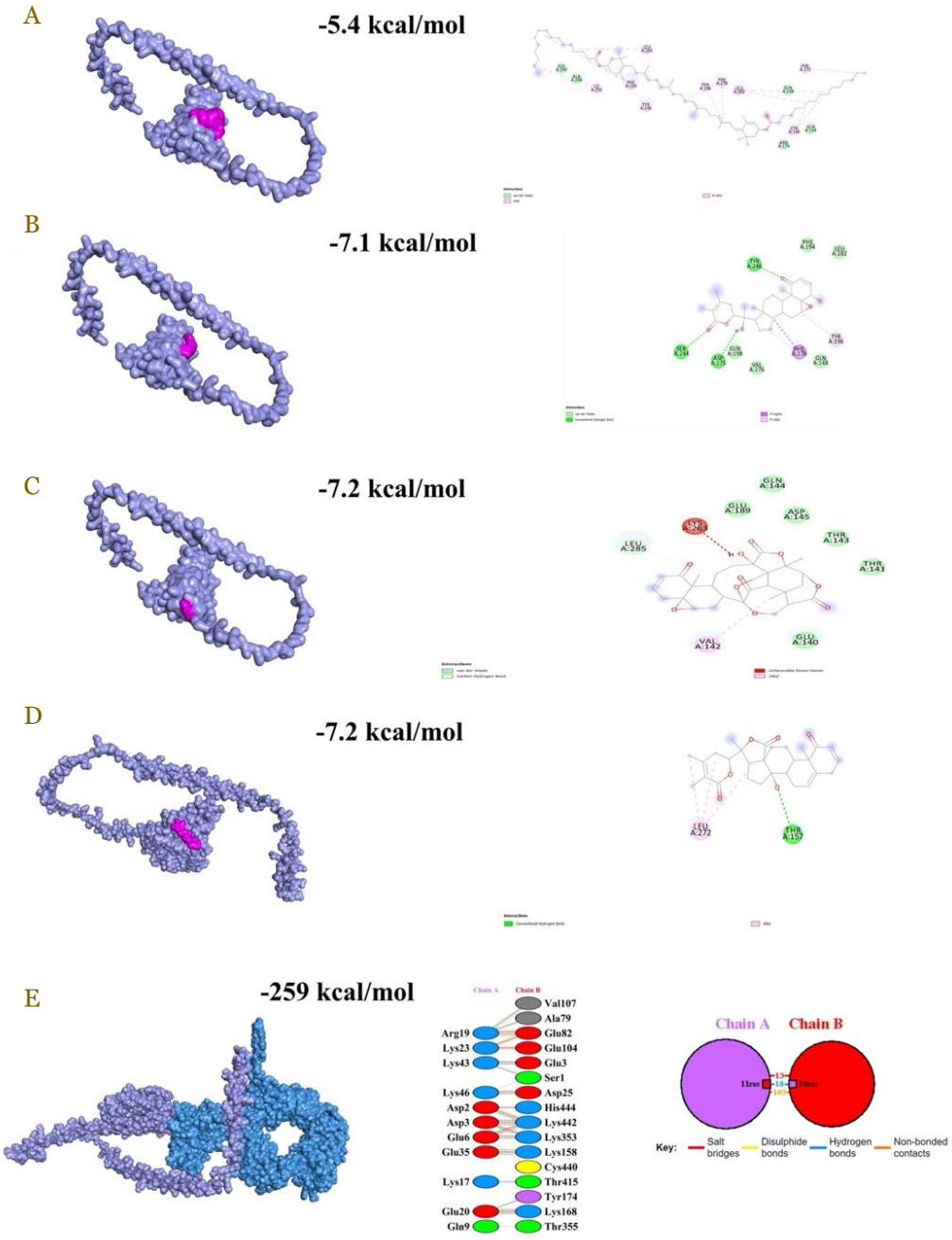

Figure 3. Molecular docking results of physalin + BAFF (A), withanolide + BAFF (B), physalin F + BAFF (C), withaphysalin A + BAFF (D), and belimumab + BAFF (E).

TACI protein

Based on the docking results of both the compounds and the control with the TACI protein (**Figure 4**), it was found that physalin F exhibited the best binding energy, which is -8.3 kcal/mol, with one hydrogen bond at GLN 99.

In the context of the control belimumab, a binding energy of -258.4 kcal/mol was obtained, with 4 salt bridges, 12 hydrogen bonds, and 86 non-bonded contacts. The number of bonds was significantly fewer compared to belimumab's interaction with the BAFF protein, as is the binding affinity. Therefore, it can be inferred that belimumab will interact primarily with the BAFF protein rather than TACI. In addition to physalin F, it is noteworthy to highlight the compound

withanolide, characterized by a binding energy of -7.1 kcal/mol, as a prospective candidate for TACI inhibition.

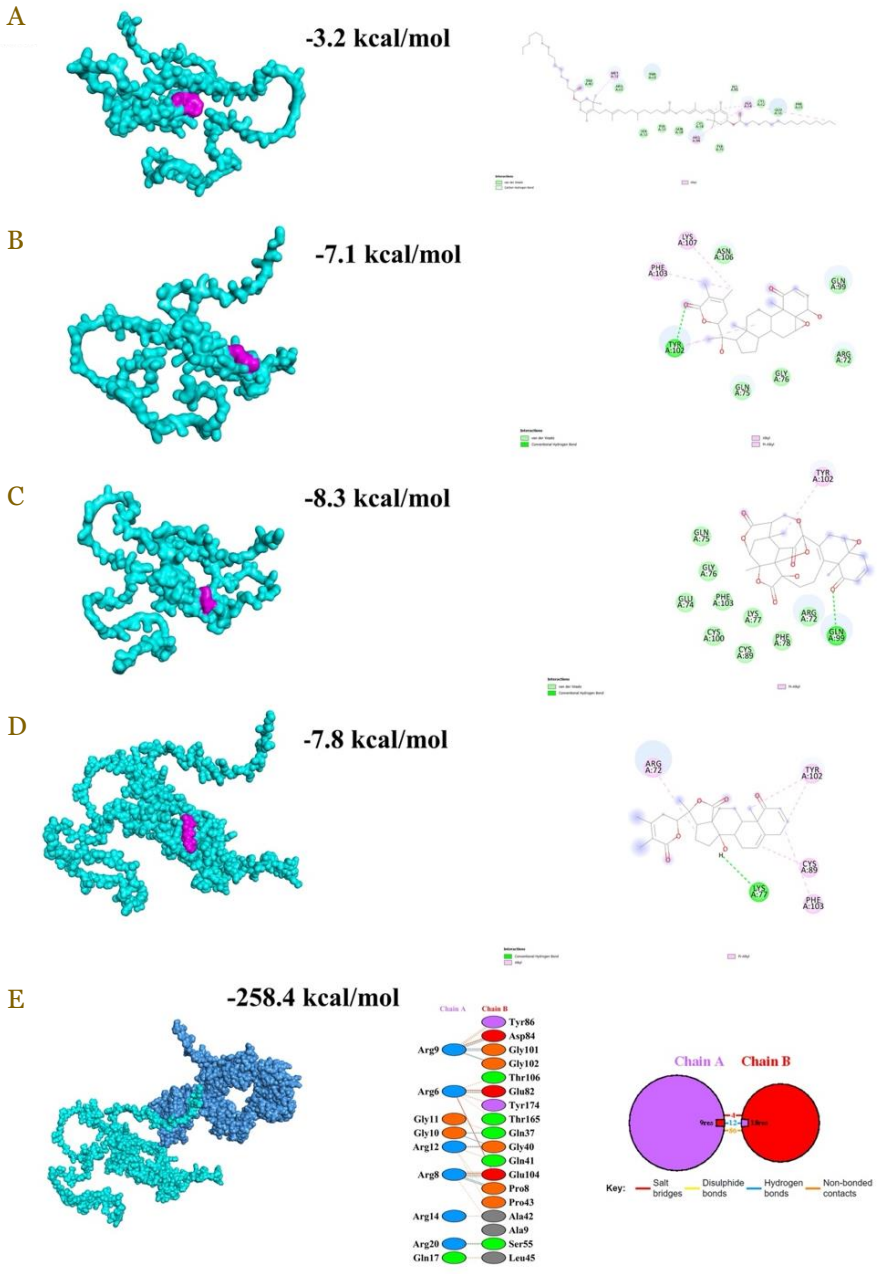

Figure 4. Molecular docking results of physalin + TACI (A), withanolide + TACI (B), physalin F + TACI (C), withaphysalin A (D), and belimumab + TACI (E).

BCMA protein

Among withanolide, physalin, physalin F, and withaphysalin A, withanolide emerged as the most promising candidate for BCMA protein inhibition (Figure 5.). Despite its binding energy of -7.0 kcal/mol, which might seem lower than that of physalin F (-7.7 kcal/mol) and withaphysalin A (-8.1 kcal/mol), the interaction with withanolide involved the formation of four hydrogen bonds with THR36, SER16, PHE14, and LEU35. Meanwhile, in the interaction between belimumab and BCMA, the system exhibited a binding energy of -242 kcal/mol, slightly lower compared to its interactions with BAFF and TACI. However, the number of bonds formed was still higher than its interaction with TACI, with 9 salt bridges, 15 hydrogen bonds, and 117 non-bonded contacts.

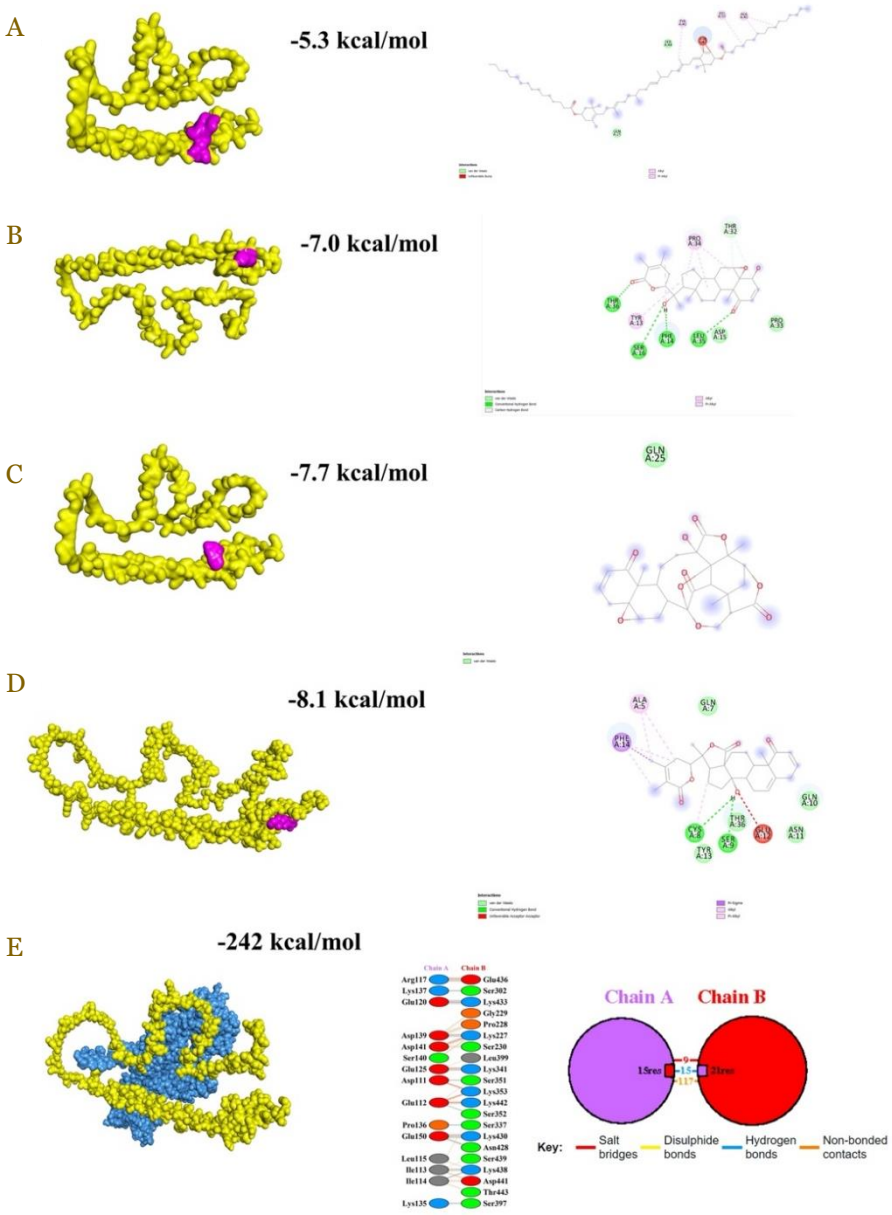

Figure 5. Molecular docking results of physalin + BCMA (A), withanolide + BCMA (B), physalin F + BCMA (C), withaphysalin A + BCMA (D), and belimumab + BCMA (E).

BAFF-R protein

In the context of BAFF-R inhibition (**Figure 6**), physalin F with -8.0 kcal/mol emerged as the most efficacious compound. This enhanced efficacy can be ascribed to its specific interactions with the protein, characterized by the formation of three hydrogen bonds with residues ARG30, ARG11, and GLY10. Furthermore, van der Waals interactions are manifested at residues LEU8, ARG9, ASP12, ALA15, and LEU27. Notably, alkyl and pi-alkyl bonds are observed in ALA13, PRO16, and PHE25.

The molecular docking data (**Supplementary data**) and other in silico analyses for withanolide A were not presented in the main paper but were available in the supplementary material. The results for withanolide A with the BAFF protein showed a binding energy of -7.3 kcal/mol. However, there are 11 unfavorable bumps interactions observed in this binding. These interactions were located at ALA 262, LEU 261, HIS 210, LEU 211, ILE 212, ILE 195, PHE 279, TYR 196, GLY 197, GLY 280, and ILE 185. On the other hand, the interaction with the BAFF-R protein and withanolide A had a binding energy of -6.8 kcal/mol, but it also exhibited three out of four interactions with unfavorable bumps. These unfavorable bumps interactions occur at LEU 91, ALA 92, and LEU 95.

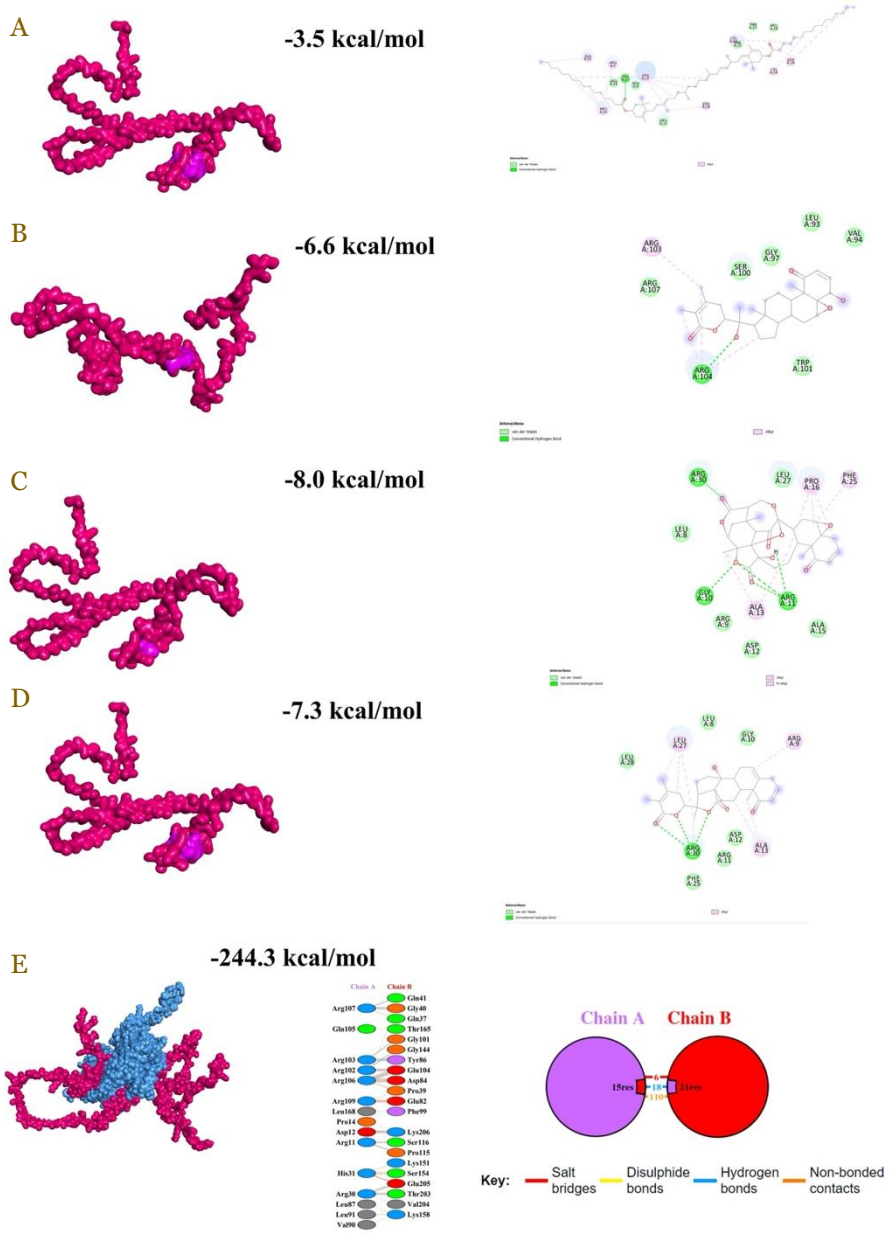

Figure 6. Molecular docking results of physalin + BAFF-R (A), withanolide + BAFF-R (B), physalin F + BAFF-R (C), withaphysalin A + BAFF-R (D), and belimumab + BAFF-R (E).

Molecular dynamic simulation analysis

TACI and physalin F complex

MD simulation was performed on the TACI and physalin F complex, where improved stability of amino acid residues of TACI was observed following the complex formation (**Figure 7**). The stability of residue 129 interacting with physalin F was improved with the change of RMSF from 5.216 Å to 3.714 Å. The increased stabilities of the protein after the complexation were observed at residue 130 (RMSF: 6.591 Å to 0.169 Å), 133 (RMSF: 11.485 Å to 5.127 Å), and 134 (RMSF: 11.769 Å to 4.969 Å).

BAFF-R and physalin F complex

The results of the molecular dynamic simulation of BAFF-R and physalin F complex are presented in **Figure 8**. Overall, the complex formation increased the stability of the protein residues. Particularly, decreased RMSFs were observed at residue 52 (from 10.609 Å to 8.649 Å), 53 (from 11.853 Å to 9.4 6 Å), 54 (from 12.697 Å to 9.31 Å), 55 (13.004 Å to 10.153 Å), 56 (from 12.706 Å to 10.123 Å), 57 (12.178 Å to 9.976 Å) and 58 (11,145 Å to 10.243 Å).

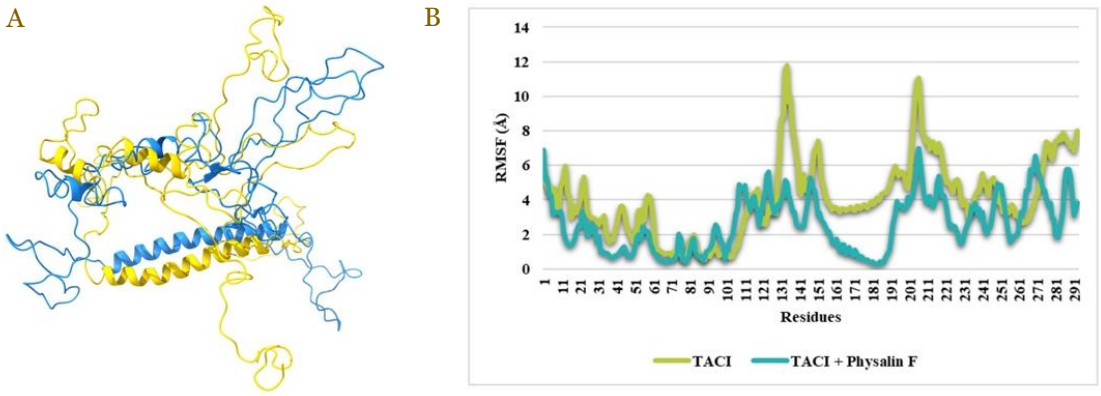

Figure 7. Three-dimensional representation of TACI—physalin F complex (blue) and native TACI (yellow) (A). Root mean square fluctuation (RMSF) of TACI—physalin F complex and native TACI from 10-ns molecular dynamic (MD) simulation (B).

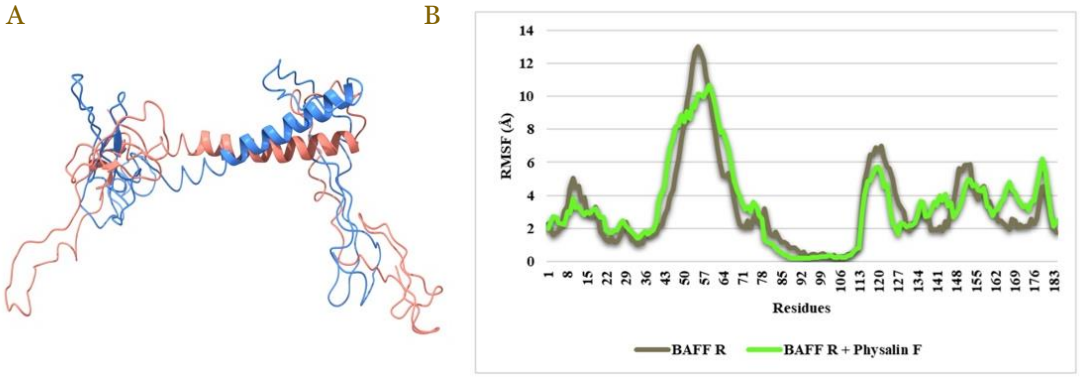

Figure 8. Three-dimensional representation of BAFF-R—physalin F complex (orange) and native BAFF-R (blue) (A). Root mean square fluctuation (RMSF) of BAFF-R —physalin F complex and native BAFF-R from 10-ns molecular dynamic (MD) simulation (B).

BAFF and withanolide complex

The 3D representation of the BAFF and withanolide complex and the RMSF recorded from the 10-ns MD simulation are presented in **Figure 9**. The improvement of general stability was not observed in this complex during the simulation. Increased RMSFs were particularly observed at residues 120 (from 7.384 Å to 11.466 Å), 121 (from 6.276 Å to 12.521 Å), 122 (from 5.056 Å to 13.225 Å), 123 (from 4.001 Å to 14.412 Å), 124 (from 3.307 Å to 14.986 Å), 125 (from 2.688 Å to 15.232 Å), 126 (from 2.441 Å to 14.984 Å), 127 (from 2.432 Å to 13.543 Å), 128 (from 2.833 Å to 11.918 Å), 129 (from 3.783 Å to 10.737 Å).

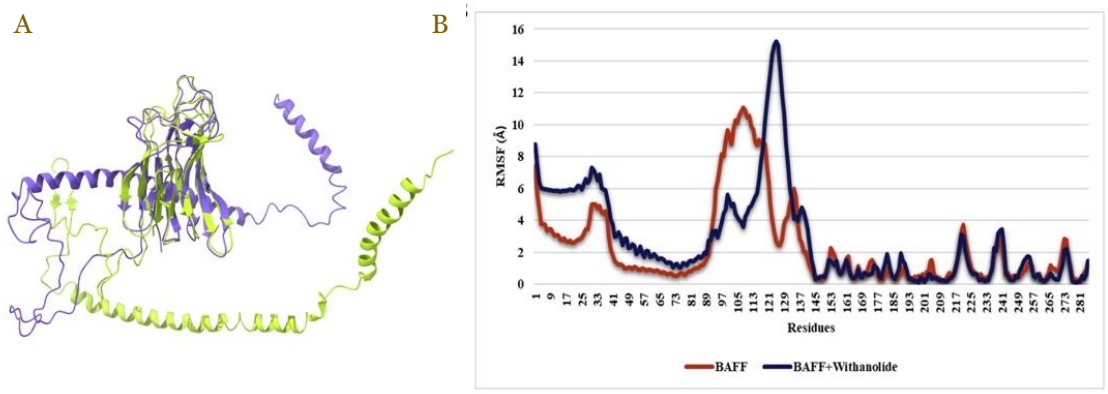

Figure 9. Three-dimensional representation of BAFF—withanolide complex (purple) and native BAFF (green) (A). Root mean square fluctuation (RMSF) of BAFF—withanolide complex and native BAFF from 10-ns molecular dynamic (MD) simulation (B).

BCMA and withanolide complex

The results of MD simulation of BCMA and withanolide complex, in comparison with native BCMA, are presented in **Figure 10**. There was no improvement found in the general stability. The RMSFs increased at the residues ranging from 113 to 183. The increased RMSFs are clearly observable at 167 (from 9.076 Å to 14.137 Å), 168 (from 9.957 Å to 13.657 Å), 169 (from 10.744 Å to 12.846 Å), 170 (from 9.667 Å to 12.482 Å), 171 (from 8.593 Å to 11.48 Å) and 172 (from 6.788 Å to 11.503 Å).

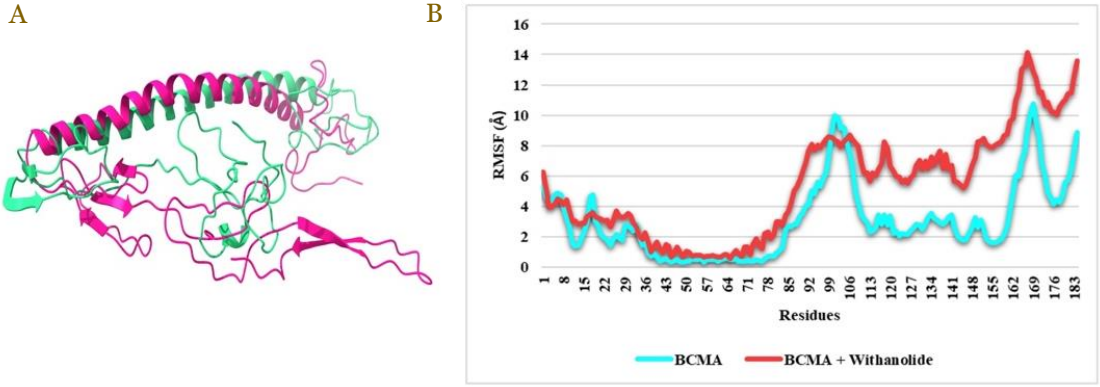

Figure 10. Three-dimensional representation of BCMA—withanolide complex (pink) and native BCMA (green) (A). Root mean square fluctuation (RMSF) of BCMA—withanolide complex and native BCMA from 10-ns molecular dynamic (MD) simulation (B).

Discussion

Bioactivity of *Physalis angulate* compounds

The immunosuppressive qualities inherent in withanolide can effectively moderate an excessively active immune system, a characteristic that holds significance in cases of autoimmune-related nephrotic syndrome. Furthermore, these compounds exhibit antioxidant properties, which play a pivotal role in reducing oxidative stress within the kidneys. By concurrently addressing immune system dysfunction and oxidative stress, withanolide provides a multifaceted approach to the management of nephrotic syndrome, potentially facilitating the protection and restoration of kidney tissues [24]. In the case of physalin, various probabilities of bioactivity have been identified that support their potential in ameliorating nephrotic syndrome. For example, they exhibit oxidoreductase inhibitor properties, which are pertinent due to the significance of reducing oxidative stress in the kidneys. Oxidative stress, characterized by an imbalance between the production of reactive oxygen species (ROS) and the body's capacity to detoxify or repair the resulting damage, significantly contributes to the progression of kidney injury in this condition. Furthermore, the recognition of physalin as an apoptosis agonist is intriguing. Apoptosis, or programmed cell death, plays a vital role in regulating cell proliferation and maintaining tissue homeostasis. In cases of nephrotic syndrome, where certain cells may over-proliferate and contribute to the disease's pathology, the ability of physalin to promote apoptosis could offer significant benefits. By inducing the controlled death of these over-proliferating cells, physalin may help restore the balance and mitigate the progression of the disease [25].

ADMET of *Physalis angulata*

The detailed analysis of specific pharmacokinetic parameters provides a nuanced understanding of the pharmaceutical potential of withanolide, withanolide A, physalin, and physalin F. The high Caco-2 permeability and efficient absorption rates observed in withanolide and physalin position them as promising candidates for pharmaceutical development. Their classification as well-absorbed compounds, favorable P-glycoprotein interactions, and non-toxic hepatotoxicity, underscores their potential safety and efficacy. It is crucial to highlight that P-glycoprotein functions as an ATP-binding cassette (ABC) transporter, acting as a biological defense mechanism that eliminates toxins and foreign substances from within cells [26]. However, the distinctive pharmacokinetic profile of physalin F, marked by exceptional absorption but potential

concerns related to negative total clearance and toxicity, necessitates careful consideration in drug development. The divergent interactions with Cytochrome P450 isoforms highlight the need for a tailored approach to understanding the metabolic pathways of these compounds [22].

Molecular modelling and assessment

Rapid advancements in computational methods for protein modelling have posed a significant challenge to various experimental approaches. Within the realm of protein structure prediction, where emerging computational algorithms often assert superior results compared to experimental models, the use of the term artificial intelligence has generated heightened enthusiasm regarding the efficacy of these tools. This enthusiasm has been particularly pronounced since the emergence of AlphaFold in 2020, marking a remarkable achievement in predicting the 3D structure of proteins with impressive accuracy. AlphaFold utilizes deep learning and neural networks to forecast the three-dimensional structure of proteins, demonstrating a high level of precision. This method has instigated substantial changes in the field of structural biology, facilitating a deeper understanding of protein functions and interactions [23]. Based on quality assessments, it has been determined that the model is promising in adhering to Ramachandran rules. The BCMA protein demonstrates favorable positioning of residues within allowed regions. Likewise, the BAFF protein exhibits high-quality modelling, with residues predominantly in favored and allowed regions. The BAFF-R protein maintains quality modelling, with a significant proportion of residues within favored and allowed regions. Despite the larger size of the TACI protein, the model retains the commendable quality, indicating a substantial portion of residues within favored and allowed regions [23].

Molecular docking analysis

The docking results with BAFF shed light on the inhibitory potential of belimumab, physalin F, and withanolide concerning the BAFF protein. Physalin F, while showing the most favorable binding energy, raised concerns due to unfavorable donor-donor interactions, suggesting potential protein instability. In contrast, withanolide emerged as a promising candidate for inhibiting the BAFF protein. The information that these binding sites do not overlap suggested that withanolide could function either independently or in combination with belimumab to inhibit the BAFF protein. This indicates that these metabolite compounds may present an additional or alternative therapeutic approach for patients already undergoing belimumab treatment, and the benefit of having distinct binding sites is the potential for a synergistic therapeutic effect [22]. Meanwhile, the docking result with TACI showed that physalin F is a prospective candidate for TACI inhibition. Physalin F has gained recognition for its formidable anti-proliferative impact on diverse tumor cells. This anti-proliferative influence is believed to originate from its capacity to disrupt the cell cycle, subsequently leading to apoptotic cell death. In the study by Yang *et al*. [26], it was also ascertained that physalin F possesses the ability to induce apoptosis in HT1080 cells, primarily through the inhibition of isocitrate dehydrogenase (IDH) enzymatic activity. Furthermore, the research reported that physalin F resulted in cell cycle arrest, accompanied by an elevation in the levels of p53 and p21, especially in renal carcinoma cells.

Furthermore, the research reported that physalin F resulted in cell cycle arrest, accompanied by an elevation in the levels of p53 and p21, especially in renal carcinoma cells. Subsequently, the docking results with the BCMA showed that withanolide appears to be the most promising contender for inhibiting the BCMA protein. Four hydrogen bonds are formed in the interaction with withanolide. Hydrogen bonds play a pivotal role in augmenting the binding affinity between a drug compound and its target, often a protein or enzyme. This augmentation can lead to a more efficient interaction and potentially result in enhanced therapeutic outcomes. Furthermore, hydrogen bonds contribute to the stability of the drug-receptor complex, reducing the likelihood of dissociation or degradation within the body before achieving the desired therapeutic effect [19,21,27].

Withanolide is a natural steroid component that forms within the ergostane framework. This key phytosteroid, primarily found throughout various parts of *Physalis angulata*, is not commonly present in most plant species. Withanolide is a specific component within the

Solanaceae family, notably in plants like Physalis, Withania, Acnistus, Dunalia, and Datura. Withanolides belong to the class of polyoxygenated steroids and are based on the C28 ergostane skeleton. They are characterized by the presence of a δ- or γ-lactone ring formed from the carboxylic group at C-26 and the oxidized hydroxyl group at C-23 or C-22 [28]. Unfavorable bump interactions indicate steric clashes or clash scores between atoms or groups, highlighting situations where these entities are positioned too closely, resulting in repulsion or adverse interactions. Such occurrences arise when atoms or groups within a molecule are placed too closely together, disregarding fundamental principles of molecular geometry, consequently creating high-energy conformations that are typically chemically disadvantageous. When compared to the general data for withanolide, it can be concluded that withanolide A is not capable of functioning as a BAFF inhibitor.

Validation through MD simulation revealed that the proteins forming complex with physalin F tend to experience an increase in stability. Meanwhile, residues of the protein were likely to be unstable after interacting with withanolides. Based on the stability observed throughout the MD simulation, physalin F can be considered a suitable inhibitor. The polyoxygenated structure of withanolides in general, including physalin and physalin F, which belong to the subfamily of withanolides with modified skeletons, leads to the incorporation of multiple oxygen functionalities into the carboxylic framework. Consequently, these compound classes are characterized by complex and diverse structural features. This structural diversity equips the active compounds derived from *Physalis angulata* with a wide range of pharmacological activities. *Physalis angulata* has been extensively researched and is recognized for its multifaceted biological effects, encompassing antimicrobial, antitumor, anti-inflammatory, and immunomodulatory properties. Therefore, withanolides in general, withaphysalin A and physalin F as a subgroup of withanolides, are considered valuable sources of bioactive constituents and promising drug candidates [26,29].

Strengths and limitations

This study represents a comprehensive exploration of potential therapeutic pathways for nephrotic syndrome, emphasizing B-cell-mediated mechanisms and innovative approaches to treatment. By integrating data mining, bioactivity analysis, ADMET profiling, molecular modelling, and molecular docking, we investigated the immunomodulatory properties of withanolides, including physalins and withaphysalin A, derived from *Physalis angulata*. Our findings highlight the potential of these compounds as inhibitors of BAFF and its receptors, suggesting novel avenues for therapeutic intervention in nephrotic syndrome. However, while our computational models demonstrate promising results, the translation of these findings into clinical applications necessitates rigorous validation through in vivo studies and clinical trials. Addressing these limitations is crucial to substantiate the efficacy, safety, and clinical relevance of *Physalis angulata* compounds in treating nephrotic syndrome, thereby advancing toward potential therapeutic implementation.

Conclusion

Nephrotic syndrome, characterized by significant proteinuria, has recently drawn attention to podocyte injury involving B-cell-mediated mechanisms, underscoring the pivotal role of B-cells in its pathogenesis. In the quest for potential therapeutic strategies, this study explored withanolides, withaphysalin A, including physalins, found in *Physalis angulata*, and belimumab, a monoclonal antibody targeting BAFF and its receptors (TACI, BCMA, and BAFF-R). Withanolides exhibited immunosuppressive and oxidoreductase inhibitor properties, potentially beneficial for managing nephrotic syndrome, while physalins and withaphysalin A, as a subgroup of withanolides, displayed antioxidative and apoptosis-inducing potential. Efficient pharmacokinetic absorption of both withanolides, withaphysalin A and physalins were observed, necessitating further research. Molecular docking studies revealed that withanolides have potential as BAFF and BCMA inhibitors, while physalin F, another component of withanolides, could act as a TACI inhibitor and a potent BAFF-R inhibitor, showcasing their diverse interactions with B-cell-related proteins. These withanolide compounds from *Physalis angulata* offer promising therapeutic avenues for nephrotic syndrome, providing alternative approaches to

target B-cells, and their structural complexity underscores their potential as valuable bioactive constituents and drug candidates, warranting further clinical exploration.

Ethics approval

Not required.

Acknowledgments

The authors acknowledge and appreciate the Research and Community Service Agency (BPPM), Faculty of Medicine, Universitas Brawijaya, for the financial support.

Competing interests

All the authors declare that there are no conflicts of interest.

Funding

PNPB funding for the Basic Research Program.

Underlying data

Supplementary data supporting the findings of this study is available from the following link: https://figshare.com/articles/journal_contribution/Supplementary_material_docx/26840875

How to cite

Kardani AK, Fitri LE, Samsu N, *et al*. Inhibition of B-cell activating factor activity using active compounds from *Physalis angulata* in the mechanism of nephrotic syndrome improvement: A computational approach. Narra J 2024; 4 (3): e859 - http://doi.org/10.52225/narra.v4i3.859.

References

1. Veltkamp F, Rensma LR, Bouts AHM, *et al*. Incidence and relapse of idiopathic nephrotic syndrome: Meta-analysis. Pediatrics 2021;148(1):1-17.
2. Forero-Delgadillo J, Ochoa V, Restrepo JM, *et al*. B-cell activating factor (BAFF) and its receptors' expression in pediatric nephrotic syndrome is associated with worse prognosis. PLoS One 2022;17(11):1-13.
3. Colucci M, Corpetti G, Emma F, *et al*. Immunology of idiopathic nephrotic syndrome. Pediatr Nephrol 2018;33(4):573-584.
4. Pescovitz MD, Greenbaum CJ, Krause-Steinrauf H, *et al*. Rituximab, B-lymphocyte depletion, and preservation of beta-cell function. N Engl J Med 2009;361(22):2143-2152.
5. Hjorten R, Anwar Z, Reidy KJ. Long-term outcomes of childhood onset nephrotic syndrome. Front Pediatr 2016;4:53.
6. Schijvens AM, Dorresteijn EM, Roeleveld N, *et al*. REducing STEroids in Relapsing Nephrotic syndrome: The RESTERN study-protocol of a national, double-blind, randomised, placebo-controlled, non-inferiority intervention study. BMJ Open 2017;7(9):e018148.
7. Hwang Y, Kim G, Kim W. Review of clinical research about herbal medicine treatment on chronic pancreatitis - Research on CNKI. J Int Korean Med 2017;38(1):48-63.
8. Jackson SW, Davidson A. BAFF inhibition in SLE - Is tolerance restored? Immunol Rev 2019;292(1):102-119.
9. Jiang Y, Tao X, Chen H. The effect of rituximab assisted prednisone and cyclophosphamide on the treatment of idiopathic membranous nephropathy and its influence on serum nephrin and BAFF levels. Pak J Zool 2021;54(2):771-776.
10. Adnyana IK, Yulinah E, Maeistuti N, *et al*. Evaluation of ethanolic extracts of mullaca (Physalis Angulata L.) herbs for treatment of lupus disease in mice induced pristane. Procedia Chem 2014;13:186-193.
11. White PT, Subramanian C, Motiwala HF, *et al*. Natural withanolides in the treatment of chronic diseases. Adv Exp Med Biol 2016;928:329-373.
12. Sheba SH, Setiani NA, Sutjiatmo AB, *et al*. Combination effect of cecendet (Physalisangulata L.) extract and methylprednisolone in reducing inflammation and improving renal functions in pristane-induced lupus rat models. Maj Kedokt Bandung 2019;51(1):17-24.

13. Soares MB, Brustolim D, Santos LA, *et al*. Physalins B, F and G, seco-steroids purified from Physalis angulata L., inhibit lymphocyte function and allogeneic transplant rejection. Int Immunopharmacol 2006;6(3):408-414.
14. Sun CP, Qiu CY, Yuan T, *et al*. Antiproliferative and anti-inflammatory withanolides from Physalis angulata. J Nat Prod 2016;79(6):1586-1597.
15. Meira CS, Soares JWC, Dos Reis BPZC, *et al*. Therapeutic applications of physalins: Powerful natural weapons. Front Pharmacol 2022;13:864714.
16. Brar R, Chand Gupta R. Phytochemical analysis of two cytotypes (2x and 4x) of Physalis angulata an important medicinal plant, collected from Rajasthan. Biochem Mol Biol J 2017;3(3):15.
17. Timotius KH, Tjajaindra A, Sudradjat SE. Potential anti-inflammation of Physalis angulata L. Int J Herb Med 2021;9(5):50-58.
18. Wibowo S, Widyarti S, Sabarudin A, *et al*. The role of astaxanthin compared with metformin in preventing glycated human serum albumin from possible unfolding: A molecular dynamic study. Asian J Pharm Clin Res 2019;12(9):276-282.
19. Wibowo S, Sumitro SB, Widyarti S. Computational study of Cu2+, Fe2+, Fe3+, Mn2+ and Mn3+ binding sites identification on HSA 4K2C. IOP Conf Ser Mater Sci Eng. 2020;833(1):012052.
20. Wicaksana A, Rachman T. Aktivitas Dan Efektivitas Antibakteri Ekstrak Daun Ciplukan (Physalis Angulata L.) Terhadap Pertumbuhan Bacillus Cereus. Husada Mahakam: Jurnal Kesehatan 2019;5(1):51-60.
21. Wibowo S, Costa J, Baratto MC, *et al*. Quantification and improvement of the dynamics of human serum albumin and glycated human serum albumin with astaxanthin/astaxanthin-metal ion complexes: Physico-chemical and computational approaches. Int J Mol Sci 2022;23(9):4771.
22. Pires DE, Blundell TL, Ascher DB. pkCSM: Predicting small-molecule pharmacokinetic and toxicity properties using graph-based signatures. J Med Chem 2015;58(9):4066-4072.
23. Skolnick J, Gao M, Zhou H, *et al*. AlphaFold 2: Why it works and its implications for understanding the relationships of protein sequence, structure, and function. J Chem Inf Model 2021;61(10):4827-4831.
24. Fujisawa H, Nakayama Y, Nakao S, *et al*. Effectiveness of immunosuppressive therapy for nephrotic syndrome in a patient with late-onset Fabry disease: A case report and literature review. BMC Nephrol 2019;20(1):469.
25. Granqvist A, Nilsson UA, Ebefors K, *et al*. Impaired glomerular and tubular antioxidative defense mechanisms in nephrotic syndrome. Am J Physiol Renal Physiol 2010;299(4):F898-F904.
26. Yang Y, Xiang K, Sun D, *et al*. Withanolides from dietary tomatillo suppress HT1080 cancer cell growth by targeting mutant IDH1. Bioorg Med Chem 2022;58:116655.
27. Wibowo S, Widyarti S, Sabarudin A, *et al*. DFT and molecular dynamics studies of astaxanthin-metal ions (Cu2+ and Zn2+) complex to prevent glycated human serum albumin from possible unfolding. Heliyon 2021;7(3):e06548.
28. Ludlow RF, Verdonk ML, Saini HK, *et al*. Detection of secondary binding sites in proteins using fragment screening. Proc Natl Acad Sci U S A 2015;112(52):15910-15915.
29. Chen J, Qiao XH, Mao JH. Immunopathogenesis of idiopathic nephrotic syndrome in children: Two sides of the coin. World J Pediatr 2021;17(2):115-122.